Supplementary Online Content

Schrantee A, Tamminga HGH, Bouziane C, et al. Age-dependent effects of methylphenidate on the human dopaminergic system in young vs adult patients with attention-deficit/hyperactivity disorder: a randomized clinical trial. Published online August 3, 2016. doi:10.1001/jamapsychiatry.2016.1572.

This supplementary material has been provided by the authors to give readers additional information about their work.

eFigure 1. Timeline

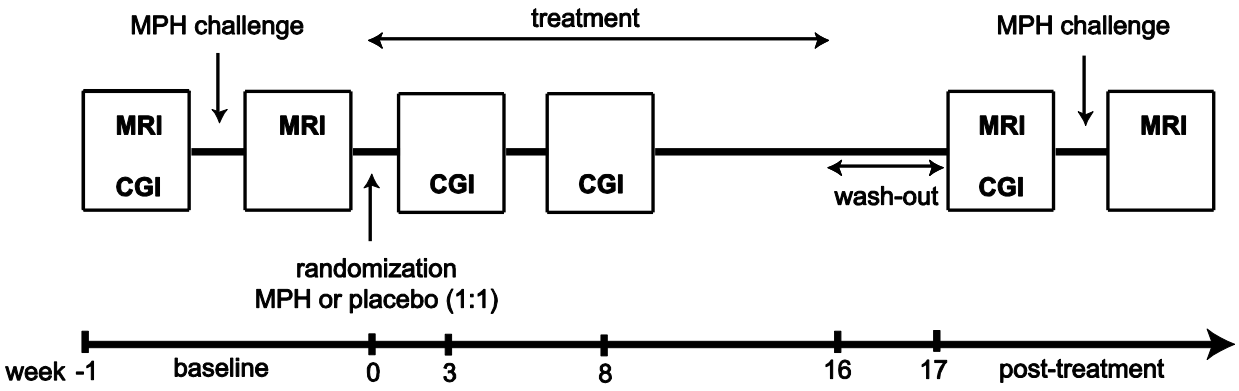

Overview of the study timeline.

eFigure 2. Regions of Interest

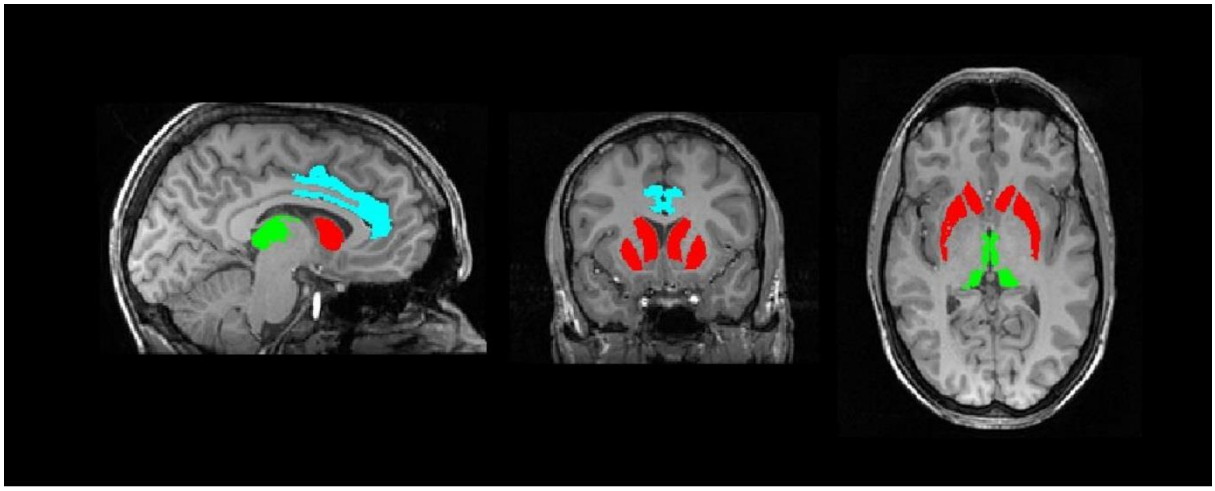

Representative T1w image with subject-specific grey matter ROIs superimposed. Red=striatum; green=thalamus blue=anterior cingulate cortex;

eFigure 3. Absolute CBF Response to MPH

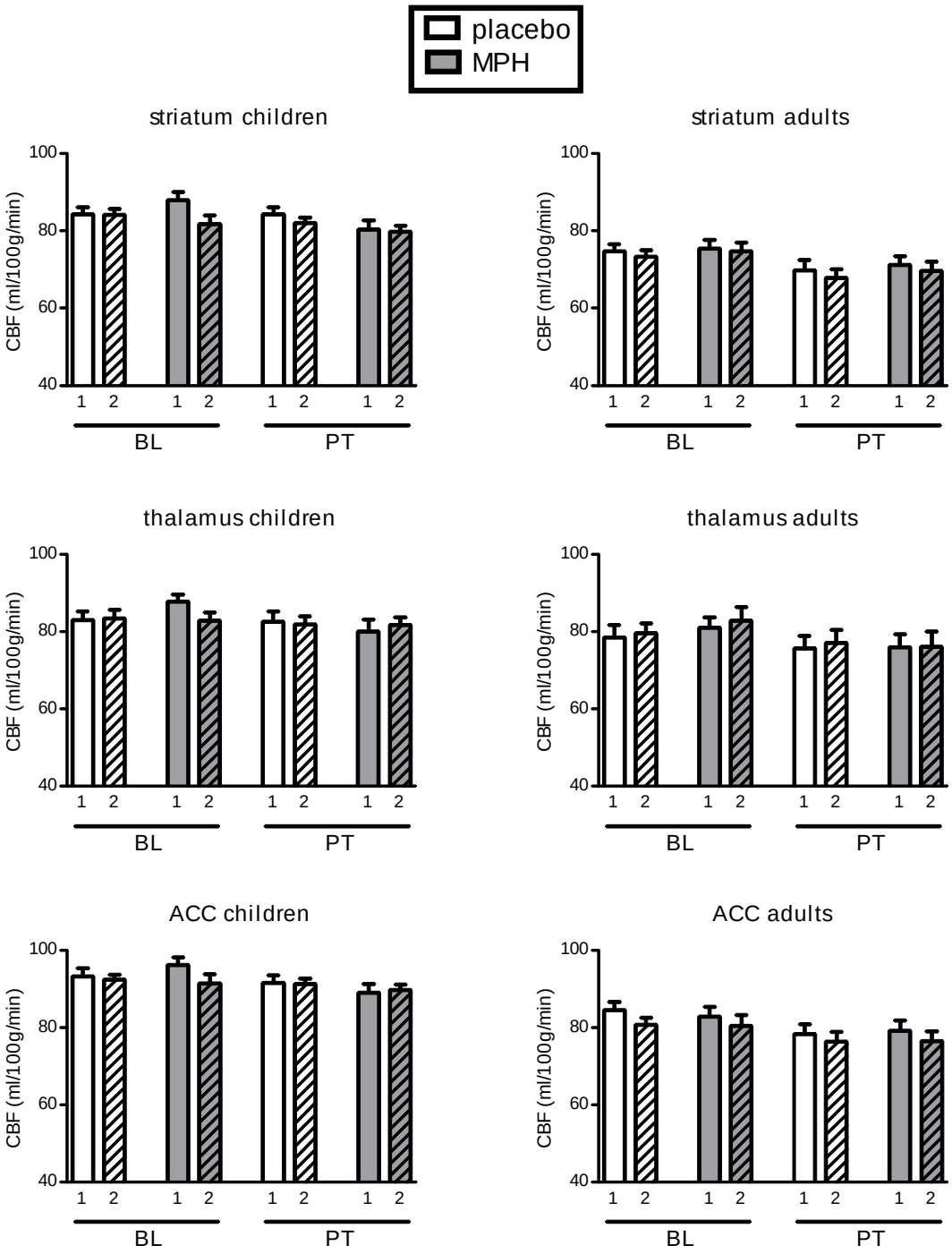

Shown are the absolute CBF values in ml/100g/min for each group at each time point. On the x-axis 1 = pre-MPH, 2 = post-MPH. Data are displayed as mean + SEM.

eFigure 4. Voxelwise Difference Maps of the Change in CBF Response to Acute MPH Challenge

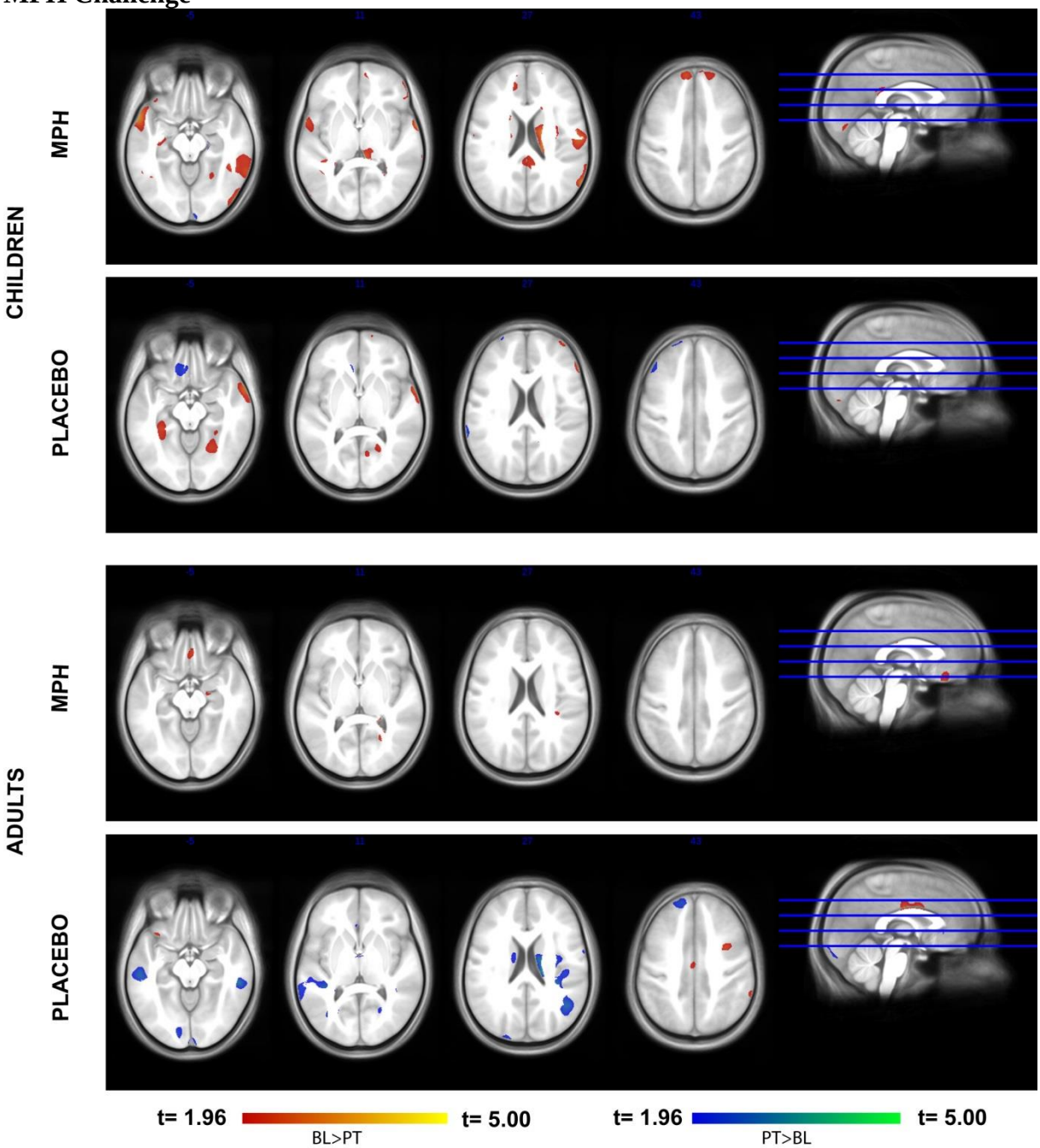

Voxel-wise difference maps of reduction in CBF from baseline and post-treatment for all groups (complete cases) of the phMRI response to MPH. Uncorrected t-stat maps are displayed thresholded at t=1.96 visualizing the difference in response to MPH and placebo treatment in children and adults.

eFigure 5. Heart Rate Response to MPH

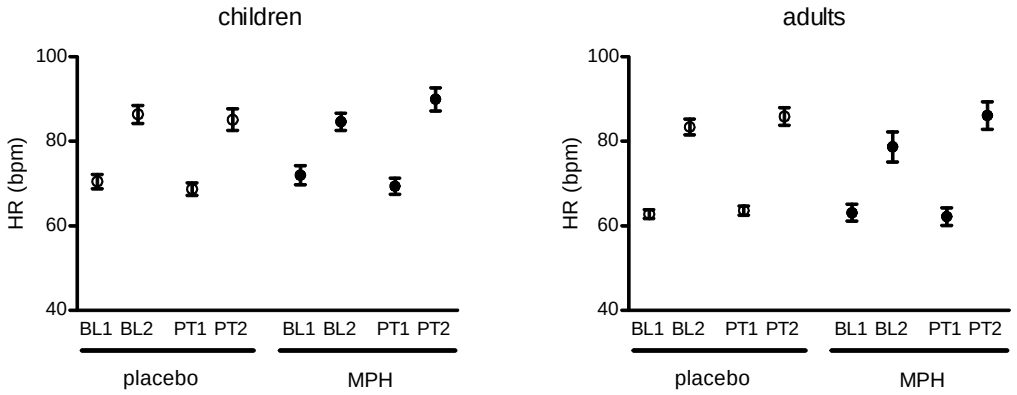

Heart rate (HR) in beats per minute (bpm) before and after MPH at baseline (BL1, B2) and post-treatment (PT1, PT2); HR differed between children and adults at baseline ($p<0.01$) and we found increased HR after acute MPH administration (children $p<0.01$; adults $p<0.01$). However, we found no age*MPH interaction at baseline ($p=0.11$), nor did MPH treatment significantly alter HR over the trial (children $p=0.25$; adults $p=0.43$).

eFigure 6. ICA Flow Response to MPH

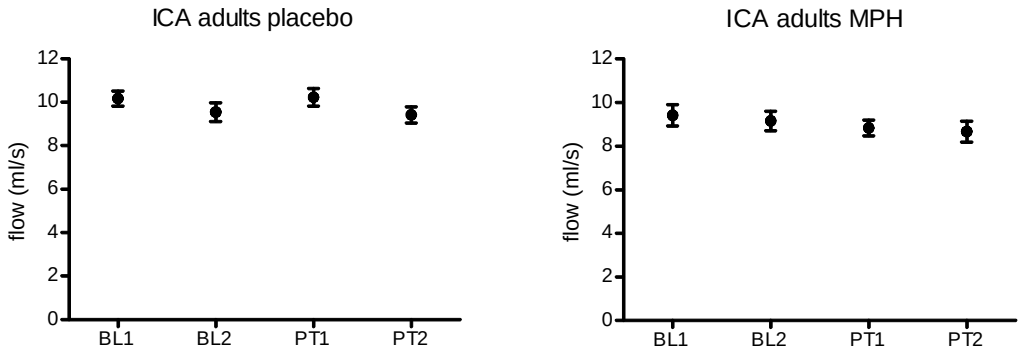

Internal carotid artery (ICA) net flow before and after MPH at baseline (BL1, B2) and post-treatment (PT1, PT2) in a subset of adult patients (N=22). The MPH challenge did not affect flow (p=0.11), nor was the response to MPH significantly different after MPH treatment (p=0.45).

eAppendix. Supplemental Appendix

Trial design and randomization

After baseline MRI assessment, patients were stratified by age and randomized to either placebo or MPH treatment (1:1). using a permuted block randomization scheme generated by the local Clinical Research Unit. The hospital pharmacy (Alkmaar) assigned participants to a specific allocation, using sequentially numbered containers. Participants as well as care providers and research personnel were blinded. The placebo tablet was identical to the MPH tablet with respect to appearance and was manufactured and labeled according to GMP guidelines (2003/94/EG). After trial commencement no significant changes were introduced to the study protocol, other than that the age-range of the adult participants was expanded from 23-30 years to 23-40 years due to inadequate inclusion rate in this age group in March 2014.

Sample size calculation

Our trial is the first study that examines DA functioning after MPH treatment in children and adults using phMRI. This means that there was only limited and indirect data available to perform a sample size calculation. Our goal for this research was to be able to detect differences in the age-dependent effect of MPH on the outgrowth of the dopaminergic system if these differences are in the magnitude of a standardized effect size of 1.25, as explained in more detail in the study protocol. To detect a standardized effect size of 1.25, a sample size of 15 patients per age group would be sufficient (two-sided significance level of 5% and a power of 90%), but to account for drop-out (including drop-out due to motion artifacts on MRI) 25 subjects in each group were included in the ePOD project. If participants dropped out of the study after randomization, they were not replaced.

phMRI acquisition and processing

phMRI data were acquired using two 3.0T Philips scanners (Achieva / Intera, Philips Medical Systems, Best, The Netherlands). CBF was measured with arterial spin labeling (ASL) MRI. A 2D gradient-echo echo-planar imaging pseudo-continuous ASL (pCASL) sequence with the following parameters was used: repetition time (TR)/echo time (TE) = 4000/14 ms; post-labeling delay = 1650 ms; label duration = 1525 ms; field-of-view (FOV) = 240x240 mm; 17 contiguous slices; 75 control-label pairs ($M_{control}$ and M_{label}); voxel size = 3x3x7 mm, no background suppression. In addition, an anatomical 3D fast field echo (FFE) T1-weighted (T1w) scan was obtained with the following scan parameters: TR/TE = 9.8/4.6; FOV = 256 x 256 x 120; voxel size = 0.875x0.875x1.2 mm.

Data were processed using the Iris pipeline for CBF quantification and multi-atlas region segmentation[1]. All image registrations were performed using Elastix registration software[2].

CBF was analyzed in GM only. To correct for patient motion, the time series were rigidly registered using a group-wise method that uses a similarity metric based on principal component analysis[3]. After motion correction, all pairs of $M_{control}$ and M_{label} images were subtracted (M_{diff}). As large motion influences the ASL signal quality, outlier

rejection was performed for the M_{diff} images. For every ASL scan, we have 75 time points, and therefore 75 M_{diff} images. For each pair of M_{diff} images, we computed the sum of squared differences (SSD) which is the sum of all squared voxel-wise differences between the two images. As such, for each of the 75 time points, we obtained 74 SSD values over which we computed the median and SD. To obtain a more robust estimate of the SD, we computed this based on only the SSD values that were lower than the median. If more than 50% of the SSD values were larger than the median+(3*SD) this timepoint was considered an outlier. If more than 15 out of 75 timepoints were outliers the complete timeseries was removed from the analysis (5% of scans). After removal of the outliers motion correction was performed on the remaining timepoints, and the resulting motion-compensated M_{diff} images were averaged to obtain a perfusion-weighted image (ΔM). The average of $M_{control}$ images was used as a proton-density normalization image (M_0) for the CBF quantification. For each subject, probabilistic GM segmentations (SPM8, Statistical Parametric Mapping, UCL, London, UK) were rigidly registered to the ΔM images by maximizing mutual information. CBF was quantified using the single-compartment model proposed by Buxton et al.[4] which is the recommended approach for pCASL[5]. The quantification accounted for post-labeling delay differences between slices due to the 2D read-out. The following parameters were used: labeling efficiency α_{GM} = 0.85, $T1_{GM}$ = 1.6ms, blood-brain partition coefficient λ_{GM} = 0.95mL/g. CBF was quantified in GM only using a 3D method for partial volume correction based on local linear regression using the tissue probability maps[6,7].

ROI-based analysis

For each participant, CBF maps were transformed to T1w space and regions of interest (ROIs) were defined using a multi-atlas approach. This involved the registration of 30 labeled T1w images[8,9], each containing 83 ROIs, with the participants' T1w images. Registration with the participants' nonuniformity-corrected T1w images[10] were performed with a rigid, affine, and a non-rigid B-spline transformation model consecutively. For this registration, both the participants' and the labeled T1w images were masked using the Brain Extraction Tool[11], these masks were also used for initialization of the registration. The labels of the 30 atlas images were fused using a majority voting algorithm to obtain a final ROI labeling[12]. For these ROIs, mean CBF values within GM were computed, which are used in our study.

Exploratory voxel-based analysis

A group template space was constructed based on the T1w images of all subjects using a procedure that avoids bias towards any of the individual T1w images[1]. In this approach, the coordinate transformations from the template space to the subject's T1w space were derived from pairwise image registrations of all pairs of T1w images. For these pairwise image registrations, we used T1w images that were non-uniformity corrected and skull-stripped using the multi-atlas brain mask explained above. The pairwise registrations were performed using a similarity, affine, and nonrigid B-spline transformation model consecutively. A similarity transformation is a rigid transformation including isotropic scaling.

CBF maps were transformed to template space in one pass by concatenating the template-T1w transformation and the inverted ASL-T1w transformation and subsequently smoothed with an 8 mm FWHM kernel. As these were exploratory analyses, complete-case analysis was used. Voxel-wise changes in CBF difference maps per session (baseline or post-treatment) were assessed non-parametrically using the Randomise toolbox in the Functional Magnetic Resonance Imaging of the Brain (FMRIB) Software Library (FSL 4.0, Oxford, UK; http://www.fmrib.ox.ac.uk/fsl). eFigure 4 shows uncorrected t-stat maps at baseline and post-treatment for all four groups, calculated using a one-sample t-test using threshold free cluster enhancement (TFCE). Using uncorrected t-stat maps we may identify additional regions with a response to MPH treatment in children, but according to protocol, we only statistically analyzed three a-priori defined ROIs.

Additional statistics Figure 2

Children, paired t-tests

Methylphenidate group. Striatum 95% CI -0.4 to 11.8; P = .07, ηp^2 = 17 0.13. ACC 95% CI -0.1 to 11.1; P = .06, ηp^2 = 0.15

Placebo group. Striatum 95% CI -1.9 to 6.0; P = 0.30 ηp2 = 0.04. Thalamus 95% CI -6.7 to 8.7; P = 0.79, ηp^2 = 0.003. ACC: 95% CI -6.4 to 5.2; P = .83, ηp^2 = 0.002.

Adults, paired t-tests

Methylphenidate group. Striatum 95% CI -2.2 to 3.6; P = 0.62, ηp^2 = 0.011. Thalamus 95% CI -4.8 to 8.2, P = 0.59, ηp^2 = 0.013. ACC 95% CI -3.1 to 3.8; P = .85, ηp^2 = 0.002

Placebo group: Striatum 95% CI -2.9 to 3.9; P = 0.78, ηp^2 = 0.004. Thalamus 95% CI -5.5 to 4.7; P = 0.87, ηp^2 = 0.001. ACC: 95% CI -6.0 to 2.1, P = .34, ηp^2 = 0.04

Relative CBF changes

Previous studies have investigated whether absolute or relative changes in CBF best represent underlying neuronal activity, bus no consensus has been reached. Therefore, we here show the statistical analyses of the relative CBF, calculated as (post-MPH – pre-MPH)/pre-MPH from baseline to post-treatment. The results are comparable to those reported in the main manuscript, with the child MPH group showing persistent changes in CBF response to MPH, whereas the other groups do not. Hence, these results do not change our conclusions.

Children, paired t-tests:

MPH group. Striatum *P*=0.06. Thalamus *P*=0.04. ACC *P*=0.05

Placebo group. Striatum *P*=0.39 Thalamus *P*=0.97 ACC: *P*=0.92

Adults, paired t-tests:

MPH group. Striatum *P*=0.65. Thalamus *P*=0.57. ACC *P*=0.81

Placebo group. Striatum *P*=0.81 Thalamus *P*=0.92 ACC: *P*=0.43

Additional outcome measures

During each of the ASL scans, heart rate (HR) was monitored using a peripheral pulse unit (PPU). Average HR per scan was calculated (results are displayed in eFigure 5). HR differed between children and adults at baseline (P<0.01) and we found increased HR after acute MPH administration (children P<0.01; adults P<0.01). However, we found no

age*MPH interaction at baseline (P=0.11), nor did MPH treatment significantly alter HR over the trial (children P=0.25 ; adults P=0.43).

In addition, blood flow in the internal carotid arteries (ICAs) was determined using 2D phase-contrast MRI at an imaging slice placed perpendicular to the ICA's with unidirectional velocity encoding (venc 80 cm/s), TE/TR/FA = 5.68 ms/15 ms/15°, NSA= 2, section thickness 4 mm, in-plane resolution = 0.45x0.45mm. ROI's were drawn on the ICA's in GTflow software and net flow (ml/s) was extracted (results are displayed in eFigure 5). The MPH challenge did not affect flow (P=0.11), nor was the response to MPH significantly different after MPH treatment (P=0.45).

Together, these results suggest that despite increased HR, MPH did not induce large changes in the blood flow to the brain, nor did these effects change after treatment. Therefore, systemic effects of MPH do not influence our results and conclusions of persistent changes in CBF response to MPH in the child MPH group.

References

1. Bron EE, Steketee RME, Houston GC, et al. Diagnostic classification of arterial spin labeling and structural MRI in presenile early stage dementia. Hum Brain Mapp 2014;35(9):4916–31.
2. Klein S, Staring M, Murphy K, Viergever MA, Pluim JPW. Elastix: a toolbox for intensity-based medical image registration. IEEE Trans Med Imaging 2010;29(1):196–205.
3. Huizinga W, Poot DHJ, Guyader J-M, et al. Non-rigid Groupwise Image Registration for Motion Compensation in Quantitative MRI [Internet]. In: Biomedical Image Registration. 2014. p. 184–93.Available from: http://link.springer.com/10.1007/978-3-319-08554-8_19
4. Buxton RB, Frank LR, Wong EC, Siewert B, Warach S, Edelman RR. A general kinetic model for quantitative perfusion imaging with arterial spin labeling. Magn Reson Med 1998;40(3):383–96.
5. Alsop DC, Detre JA, Golay X, et al. Recommended implementation of arterial spin-labeled perfusion MRI for clinical applications: A consensus of the ISMRM perfusion study group and the European consortium for ASL in dementia. Magn Reson Med Off J Soc Magn Reson Med 2014;73(1):102–16.
6. Asllani I, Borogovac A, Brown TR. Regression algorithm correcting for partial volume effects in arterial spin labeling MRI. Magn Reson Med 2008;60(6):1362–71.
7. Oliver RA, Thomas DL, Golay X. Improved partial volume correction of ASL images using 3D kernels. In: ISMRM British Chapter. 2012.
8. Gousias IS, Rueckert D, Heckemann RA, et al. Automatic segmentation of brain MRIs of 2-year-olds into 83 regions of interest. Neuroimage 2008;40:672–84.
9. Hammers A, Allom R, Koepp MJ, et al. Three-dimensional maximum probability atlas of the human brain, with particular reference to the temporal lobe. Hum Brain Mapp 2003;19:224–47.

10. Tustison NJ, Avants BB, Cook PA, et al. N4ITK: improved N3 bias correction. IEEE Trans Med Imag 2010;29(6):1310–20.

11. Smith SM. Fast robust automated brain extraction. Hum Brain Mapp 2002;17(3):143–55.

12. Heckemann RA, Hajnal J V, Aljabar P, Rueckert D, Hammers A. Automatic anatomical brain MRI segmentation combining label propagation and decision fusion. Neuroimage 2006;33(1):115–26.